Turbulent Separation Avoidance for Tail-Loaded Fully Cavitating Hydrofoil Sections

Blaine R. Parkin*
The Pennsylvania State University, State College, Pa.

This paper presents a method for prescribing pressure distributions which use a Stratford pressure recovery on parts of the wetted surfaces of fully cavitating hydrofoil sections. These pressure distributions are then used in an inverse design method at the ideal attack angle (shockless entry). Such pressure distributions are most useful for tail-loaded profiles because they permit the most rapid pressure rise possible with an attached turbulent boundary layer. Examples are presented which show that very rapid pressure rises can be employed for such profiles. It is concluded that one can design practical profiles which have heavily loaded trailing edges without inducing turbulent separation.

Nomenclature

C_D = section drag coefficient
C_L = section lift coefficient
C_M = section moment coefficient
C_p = pressure coefficient
$\bar{C}_p$ = canonical pressure distribution
D = section drag force
h = magnitude of peak pressure prescribed on wetted surface
K = cavitation number
ℓ = cavity length
L = section lift force
M = section pitching moment
P_k = cavity pressure
P_0 = pressure at X_0, at the start of Stratford pressure rise
p_0 = perturbation pressure at X_0
$P(X,Y)$ = static pressure at the point X,Y
$p(X,Y)$ = perturbation pressure coefficient
P_∞ = freestream static pressure
q_c = magnitude of velocity on cavity surface
Re = Reynolds number based on chord length
Re_0 = Reynolds number based on distance X_0
S = peak pressure location measured from wetted surface trailing edge
s = peak pressure location measured from profile nose
T = cavity thickness, measured at the trailing edge of the wetted surface
U = x component of velocity vector
U_0 = flow velocity at X_0, at the start of Stratford pressure rise
U_∞ = freestream velocity
u = x component of perturbation velocity
X = coordinate along profile chord, measured from nose
x = chordwise coordinate for boundary-layer considerations
x_0 = value of x when $X = X_0$
Y = coordinate axis normal to X
Z = value of x/x_0 corresponding to $X = 1 - S$
z = normalized boundary-layer coordinate x/x_0
z_0 = value of z corresponding to $\bar{C}_p = 4/7$
α = angle of attack
λ = fraction of prescribed peak pressure
ρ = liquid density
τ = the ratio X_0/x_0

Received April 4, 1977; revision received Aug. 29, 1977.

Index categories: Boundary Layers and Convective Heat Transfer-Turbulent; Hydrodynamics; Marine Hydrodynamics, Vessel and Control Surface.

*Director of the Garfield Thomas Water Tunnel, Applied Research Laboratory and Professor of Aerospace Engineering. Associate Fellow AIAA.

Introduction

WHEN cavity thickness constraints are specifically accounted for in their design,[1,2] fully cavitating hydrofoil sections most often have the best L/D if the center of pressure on the wetted surface is as near to the profile nose as possible. Even so, there may be some situations when tail loading may be desired. Then it is necessary to make certain that turbulent separation will not occur from the very beginning of the design process.

In particular, if one specifies the cavitation number, the Reynolds number, the cavity thickness, and the profile lift coefficient, he may still need to know how to prescribe the pressure distribution so as to locate the center of pressure as close as possible to the trailing edge and still maintain attached flow on the profile wetted surface. In order to move the center of pressure to the rear, one needs to specify adverse pressure gradients on the wetted surface which become steeper and steeper as the center of pressure moves aft. The pressure distribution on the profile of Fig. 1 illustrates this situation.

It is the avoidance of turbulent separation along with other design factors just noted which has led to the following considerations. For nose-loaded profiles such considerations are probably not advantageous. For our purposes the problem of turbulent-separation avoidance was solved by B.S. Stratford in 1959.[3,4] He has given the form of the steepest pressure rise in a turbulent boundary layer which is just on the

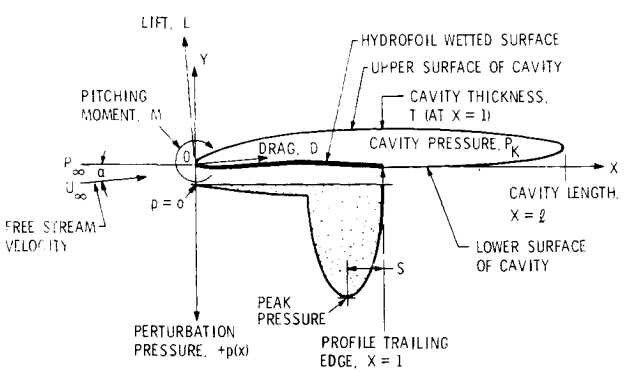

Fig. 1 General flow configuration and important design parameters for a fully cavitating hydrofoil at the ideal attack angle.

verge of separation during the whole time that a typical boundary-layer fluid particle experiences a rising pressure. Although such a boundary-layer flow is a very special one, it obviously has great technical interest, because it is not possible to prescribe steeper pressure increases without producing turbulent separation. Of equal importance for applications, Stratford was able to produce such flows experimentally and to measure the important boundary-layer flow quantities.

Since Stratford's pioneering efforts, his results have been applied in this country, principally by engineers at Douglas,[5-8] to the design of very efficient high-lift airfoils. Moreover, they have verified the correctness of their design methods in a series of wind-tunnel tests which showed excellent agreement between calculated and measured performance. On the basis of these results, there is reason to believe that the work of Stratford can be applied to the hydrodynamic design of certain supercavitating hydrofoils.

On the other hand, the design considerations appropriate to cavity flows are somewhat different from those for airfoils. Therefore, it is necessary for us to adapt some of the methods of Stratford and of Liebeck to the present inverse preliminary design procedure.[2] In this discussion, we consider profiles designed for the ideal attack angle or shockless entry (first profile design procedure[1]).

Some Preliminaries

The two-dimensional cavity flow around a hydrofoil section is illustrated schematically in Fig. 1. The liquid is incompressible and its density is ρ. The freestream velocity is U_∞ and it is inclined with respect to the profile chordline at an angle α. In this paper the attack angle α is assumed to be the ideal angle corresponding to the so-called shockless entry. The wetted surface is taken to have unit chord. The cavity thickness at the trailing edge, $X=1$, is T. The cavity length ℓ is measured from the profile nose as shown in Fig. 1. The freestream static pressure is P_∞, and the cavity pressure P_k is another constant which characterizes the cavity flow. The cavity pressure is the lowest pressure in the entire flowfield.

The cavitation number for the flow is defined by

$$K=\frac{P_\infty - P_k}{\tfrac{1}{2}\rho U_\infty{}^2}$$

If the static pressure at any point in the flow is $P(X,Y)$, we shall define the perturbation pressure (coefficient) as

$$p(X,Y)=\frac{P(X,Y)-P_k}{\tfrac{1}{2}\rho U_\infty^2}$$

with the understanding that at points on the wetted surface we have $p(X,0)=p(X)$, where now $0\le X\le 1$. On the upper and lower surfaces of the cavity, $p(X,Y)=0$. The peak pressure location is at $X=1-S$ where S is measured from the trailing edge of the wetted surface as shown in Fig. 1.

Also illustrated in Fig. 1 are the hydrodynamic forces of lift L, drag D, and pitching moment M, about the nose of the profile. The positive directions for these quantities are defined as shown. For a unit chord, we can define the force coefficients as

$$C_L=\frac{L}{\tfrac{1}{2}\rho U_\infty{}^2}$$

$$C_D=\frac{D}{\tfrac{1}{2}\rho U_\infty^2}$$

and

$$C_M=\frac{M}{\tfrac{1}{2}\rho U_\infty^2}$$

In this paper we confine our attention to the cavity drag. We shall exclude the contribution of skin friction on the wetted surface. In the present design procedure, since the Reynolds number for the flow is prescribed, the skin-friction drag can be estimated and added to the cavity drag in order to calculate the total drag force. Although the skin-friction drag can influence values of the lift-to-drag ratio, generally, the major part of the drag is cavity drag and this is the factor which is most important for comparison of competing supercavitating hydrofoil designs. Of course, if one can arrange to use the Stratford pressure rise over a significant part of the wetted surface the contribution of skin friction to the total drag can be reduced, but this cannot often be accomplished. In some special cases this fact might make the use of families of pressure distributions described here of value for practical design of nose-loaded as well as of tail-loaded supercavitating hydrofoil sections. On the other hand, alternative means of separation avoidance[9] might also be useful for controlling skin-friction drag. Whether or not such further considerations can be of practical benefit is a subject for future investigation.

In our linearized profile design procedure[1] we specify the cavitation number K, the lift coefficient C_L, the cavity thickness parameter T, the Reynolds number Re, and the perturbation pressure distribution $p(X)$ on the wetted surface. Subsequent calculations give the cavity-drag coefficient C_D, the moment coefficient C_M, the lift-to-drag ratio L/D, the ideal attack angle α, the cavity length ℓ, the wetted-surface shape $\eta(X)$, measured as ordinates with respect to the profile chordline, and the contour of the upper surface of the cavity between the profile nose and the wetted-surface trailing edge. In this paper we will not discuss this inverse design procedure. Detailed discussions of it are given elsewhere. Our aim is to show how one can derive pressure distributions for tail-loaded profiles which use Stratford recovery regions of strong adverse pressure gradient. The paper concludes with some examples of hydrodynamic performance and profile geometry which result from the use of such pressure distributions.

Prescribed Pressure Distribution

Figure 2 shows schematically the kind of pressure distribution under study. As noted already, the wetted surface of the hydrofoil is of unit chord, and it lies on the X axis as shown. Not shown in this figure are the upper surface of the cavity which originates at the profile nose and the lower surface of the cavity which leaves the profile trailing edge at $X=1$. The pressure coefficient C_P, on the wetted surface can be written in terms of the disturbance $p(X)$ and the cavitation number as

$$C_p=\frac{P(X)-P_\infty}{\tfrac{1}{2}\rho U_\infty}=-K+p(X)$$

Note that $p(X)=0$ on the cavity. Moreover, the velocity magnitude on the cavity is

$$q_c=U_\infty\sqrt{1+K}$$

and, if all disturbance velocities (u,v) are normalized with respect to this cavity speed, we can write the x component of velocity as

$$U(X)=q_c[1+u(X)]$$

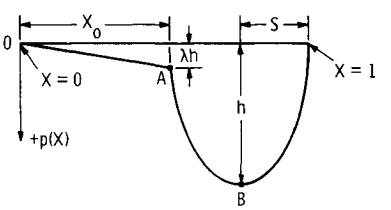

Fig. 2 The prescribed pressure distribution and characteristic parameters.

The linearized Bernoulli equation can now be written as

$$p(X) = -2(1+K)u(X)$$

We can now discuss the pressure distribution of Fig. 2 in terms of the geometric quantities it defines. Note that this diagram shows three regions:

1) From $X=0$ to $X=X_0$ at A, where $p(X_0)=\lambda h$, $\lambda \ll 1$. Two shapes for this region are considered:

$$p(X) = \lambda h(X/X_0) \qquad \text{linear rise} \qquad (1a)$$

or

$$p(X) = \lambda h\sqrt{X/X_0} \qquad \text{parabolic rise} \qquad (1b)$$

This region of small positive perturbation pressure is required to give the profiles resulting from the design procedure some tolerance to angle-of-attack variations without wetted-surface cavitation.†

2) From A to B $[X_0 \le X \le (1-S)]$, "Stratford Recovery" region. This is considered more fully later.

3) From B to the tail $[(1-S) \le X \le 1]$. This region of falling pressure will have an elliptic contour:

$$p(X) = (h/S)\sqrt{(1-X)(2S-1+X)} \qquad (2)$$

This particular shape has been chosen to have zero slope at B, where $p=h$, and to behave like $p \sim \sqrt{1-X}$ near the trailing edge. This latter condition characterizes the trailing-edge condition of the flows studied in Ref. 1.

Canonical Pressure Distribution

For boundary-layer calculations in the Stratford region, the so-called canonical pressure distribution is most useful. It is based on the pressure at $A, P_0 = P(X_0)$, just at the start of the Stratford pressure rise. Note that this definition varies somewhat from airfoil[5-8] usage in which P_0 is taken to be the *lowest* pressure on the foil. Our definition is consistent with the requirement that, except for the leading and trailing edges, the wetted surface of the profile must have a positive perturbation pressure. The canonical pressure distribution is defined as follows:

$$\bar{C}_p = \frac{P(X)-P_0}{\tfrac{1}{2}\rho U_0^2}$$

The velocity component U_0 is defined by the value of U at A, $U_0 = U(X_0)$. We can now write the canonical pressure distribution in terms of quantities which we will need for hydrofoil design. Thus,

$$\bar{C}_p = \left[\frac{P(X)-P_c}{\tfrac{1}{2}\rho U_\infty^2} + \frac{P_c-P_0}{\tfrac{1}{2}\rho U_\infty^2}\right]\frac{U_\infty^2}{U_0^2} = [p(X)-p_0]\frac{U_\infty^2}{U_0^2}$$

where p_0 is the dimensionless perturbation pressure at $X=X_0$ and $p(X)$ is the same quantity at any point X. Moreover,

$$\frac{U_\infty^2}{U_0^2} = \frac{U_\infty^2}{q_c^2[1+u(X_0)]^2} = \frac{1}{(1+K)[1-p_0/2(1+K)]^2}$$

$$= \frac{1}{1+K-p_0-p_0^2/4(1+K)}$$

†For practical applications of the method, better results are likely to be obtained with the parabolic rise than with the linear rise. Moreover, the value of λ should be chosen in accordance with an appropriate sea-state requirement. In the examples of the method considered here we will use the linear pressure rise for simplicity. The value of λ has been selected only to have a small effect on the profile lift-to-drag ratio.[1,2] No sea-state analysis was undertaken. The utility of the methods of the present paper should not be impaired by this rather arbitrary selection of illustrative examples.

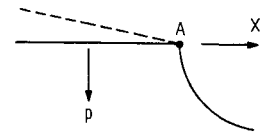

Fig. 3 The starting point for the canonical pressure distribution at A when preceded by a constant pressure region (solid line) or by an increasing pressure (dashed line).

But $1 > p_0 > p_0^2/4(1+K)$ and we can neglect the second-order term compared to 1. Moreover, in the present case $p_0 = \lambda h$. So, the final result which we require in order to translate specifications on perturbation pressure $p(X)$ into canonical pressure distributions $\bar{C}_p(X)$, is

$$\bar{C}_p(X) = \frac{p(X)-\lambda h}{1+K-\lambda h} \qquad (3)$$

The perturbation pressure is needed to calculate the lift coefficient C_L, and the canonical pressure coefficient is needed for boundary-layer calculations

Following Stratford we introduce a second streamwise coordinate x, on the wetted surface. This coordinate is positive in the direction of flow and it is associated with the canonical pressure distribution. We will relate this coordinate to the geometric coordinate X later. Now, the boundary-layer flow state at the start of the Stratford recovery is characterized by the momentum thickness at point A where $X=X_0$ and $x=x_0$. Moreover, Stratford's experiments and theory pertain to a pressure recovery region which is preceded by a flat region upstream of the point A as illustrated by the solid line in Fig. 3. In the pressure recovery region normalized boundary-layer coordinates are x/x_0 with origin at $x=0$, upstream of A. To start the pressure rise, Stratford gives formulas, based on matching the momentum thickness at $x/x_0 = 1$, to account for other than flat pressure distributions ahead of X_0 as suggested by the dashed line in Fig. 3 for both laminar and turbulent boundary layers. In the present application, we assume that the boundary layer is turbulent from the nose of the foil to the point X_0. Then, the "effective" flat region x_0 is

$$x_0 = \int_0^{X_0}\left(\frac{U}{U_0}\right)^3 dX = \int_0^{X_0}\left(\frac{2(1+K)-p(X)}{2(1+K)-p_0}\right)dX \qquad (4)$$

Then from Eqs. (1) we have for the linear pressure distribution,

$$x_0 = X_0\left[1+\frac{3}{4}\frac{\lambda h}{1+K}+\frac{5}{8}\left(\frac{\lambda h}{1+K}\right)^2+\cdots\right]$$

and we have for the parabolic nose pressure,

$$x_0 = X_0\left[1+\frac{1}{2}\frac{\lambda h}{1+K}+\frac{3}{2}\left(\frac{\lambda h}{1+K}\right)^2+\cdots\right]$$

In either of these cases, we can write

$$x_0 = X_0(1/\tau) \qquad (5)$$

The quantity τ is defined by one or the other of the foregoing functions of $\lambda h/(1+K)$.

Stratford Pressure Rise

The chief result of Stratford's investigation is contained in his canonical pressure distribution.[3,4] It is

$$\bar{C}_p\left(\frac{x}{x_0}\right) = \begin{cases} 0.49\left\{Re_0^{1/5}\left[\left(\frac{x}{x_0}\right)^{1/5}-1\right]\right\}^{1/3}, & \bar{C}_p \le \frac{4}{7} \\ 1-\frac{a}{\sqrt{(x/x_0)+b}}, & \bar{C}_p > \frac{4}{7} \end{cases} \qquad (6)$$

where

$$Re_0 = \frac{U_0 x_0}{\upsilon} = \frac{U_\infty X_0}{\upsilon}\frac{\sqrt{1+K}}{\tau}$$

and where the constants a and b are chosen to match $\bar{C}_p$ and $d\bar{C}_p/dx$ when $\bar{C}_p = 4/7$. Now, the preceding formulas are written for a hydrofoil of unit chord. Naturally, we will be dealing with foils of chord c. All we need to relate Re_0 for this case to the Reynolds number based on chord c is to put

$$Re_0 = \left(\frac{U_\infty c}{\upsilon}\right)\frac{X_0\sqrt{1+K}}{\tau} = Re\frac{X_0\sqrt{1+K}}{\tau} \tag{7}$$

where now, Re and Re_0 are based on actual distances.

Coordinates and Lift Coefficient

As we have seen, there are two sets of coordinates: those which measure actual distances along the unit chord of the profile, designated by X, X_0 etc., and those which relate to the canonical pressure distribution, designated by x, x_0, etc. We must determine the relationships between these coordinates. We have already obtained one result in the form of the Eq. (5) which is $X_0 = x_0\tau$. However, this relationship holds only at the point A on the foil; that is, when $X = (1-S)$. Moreover, at B we know that $p(X) = h$, and so the canonical pressure coefficient from Eq. (3) is

$$\bar{C}_p = \frac{(1-\lambda)h}{1+K-\lambda h} \tag{8}$$

at B. This value of C_p can be put into the Stratford recovery Eq. (6) and the corresponding value of x/x_0 found. Denote this value of x/x_0, corresponding to $X = 1-S$, by Z. Then, we find that

$$Z = \begin{cases} \left\{1 + \dfrac{1}{(Re_0)^{1/5}}\left[\dfrac{(1-\lambda)h}{0.49(1+K-\lambda h)}\right]^3\right\}^5, & \dfrac{(1-\lambda)h}{1+K-\lambda h} \le \dfrac{4}{7} \\ \left[\dfrac{a}{1-\dfrac{(1-\lambda)h}{1+K-\lambda h}}\right]^2 - b, & \dfrac{(1-\lambda)h}{1+K-\lambda h} > \dfrac{4}{7} \end{cases} \tag{9}$$

We now have two pairs of corresponding points:

at A: $x/x_0 = 1$, $X/X_0 = 1$ and
at B: $x/x_0 = Z$, $X/X_0 = (1-S)/X_0$.

Evidently, as one traverses the distance from A to B on the wetted surface, x goes from x_0 to Zx_0. Therefore, the distance traversed is $(Z-1)x_0 = (Z-1)X_0/\tau$. But, the profile has unit chord. Hence, the sum of the distances from 0 to A, A to the trailing edge is

$$1 = X_0 + (Z-1)X_0/\tau + S$$

or

$$(1-S)\tau = (\tau + Z - 1)X_0 \tag{10}$$

This is a fundamental geometrical constraint on the variables of the problem which we will need later.

In order to consider further the relationship between the boundary-layer coordinate x and the hydrofoil coordinate X, let us take a point Q in the Stratford recovery region between A and B. Suppose Q has the foil coordinate X and the boundary-layer coordinate x. Then it must follow that $X - X_0 = x - x_0$.

Now we can divide this relationship by x_0: $(X/x_0) - (X_0/x_0) = (x/x_0) - 1$. Next, we can apply Eq. (5) to this result and obtain

$$\frac{x}{x_0} = \frac{X}{x_0} + 1 - \tau \tag{11}$$

Equation (11) relates the boundary-layer variable $z = x/x_0$, appearing in the Stratford recovery equations, to the geometric coordinate X on the profile.

It is the coordinate X, along with the perturbation pressure $p(X)$, which allows us to calculate the lift coefficient. Moreover, since the quantity x_0 is determined by either of Eqs. (1) and Eq. (5), we can use Eq. (5) to relate the boundary-layer coordinate in the Stratford region to the geometric coordinate X without ambiguity. In particular, we can write

$$C_L = \int_0^1 p(X)\,dX$$

Then, with the help of Eqs. (1,2, and 3), this formula becomes

$$C_L = \lambda h\left[1 - S - \frac{1}{2}X_0\right] + \frac{\pi Sh}{4} + (1+K-\lambda h) \times \frac{X_0}{\tau}\int_\tau^{\tau+Z-1} \bar{C}_p\left(\frac{X}{x_0} + 1 - \tau\right)d\left(\frac{X}{x_0}\right) \tag{12}$$

for the linear nose pressure distribution. For the parabolic case,

$$C_L = \lambda h\left[1 - S - \frac{1}{3}X_0\right] + \frac{\pi Sh}{4} + (1+K-\lambda h) \times \frac{X_0}{\tau}\int_\tau^{\tau+Z-1} \bar{C}_p\left(\frac{X}{x_0} + 1 - \tau\right)d\left(\frac{X}{x_0}\right) \tag{13}$$

Note that Eq. (11) and the considerations leading to Eq. (10) have been used to put the integrals in Eqs. (12) and (13) in a form suitable for direct use of the Stratford recovery as specified by Eqs. (6).

Further Details of the Solution

The preceding sections provide all of the ingredients necessary for the determination of the prescribed pressure distribution on the profile. However, in order to implement these results, a number of subsidiary calculations must be completed. For example, we have noted that the Stratford recovery requires a joining of profile shapes at $\bar{C}_p = 4/7$. At this pressure, $\bar{C}_p(z)$ and $d\bar{C}_p/dz$ are to be continuous. These two conditions permit us to calculate the constants a and b of Eqs. (6). At the point of joining, let us put $z = z_0$ for $\bar{C}_p = 4/7$. Then, from the first of Eqs. (6), we have,

$$z_0 = \left[\frac{1.586}{(Re_0)^{1/5}}\right]^5$$

Next, it follows that

$$a = \frac{1.206}{Re_0^{1/5}} z_0^{4/5}(z_0^{1/5} - 1)^{2/3}$$

$$b = \frac{6.563 z_0^{4/5}(z_0^{1/5} - 1)^{2/3}}{Re_0^{1/5}} - z_0$$

Now, we can continue with the determination of the matching of the Stratford recovery to other prescribed conditions on the pressure distribution. We will require that the lift coefficient be specified in advance. We shall also specify a family of pressure distributions, depending on the

parameter S which locates the peak pressure along the chord. Members of this family will all have the same values of C_L, K, and Reynolds number. However, the point X_0 is as yet undetermined, and the value of h, the maximum pressure on the wetted surface, is also unknown.

The values X_0 and h must be determined by trial and error. We can use the basic geometrical constraint, Eq. (10), and either of Eqs. (12) or (13) for C_L to guide the iteration in a Newton-Raphson procedure. Thus, we can write Eq. (10) as

$$G(X_0,h) = \frac{1-S}{X_0} - 1 - \frac{Z-1}{\tau} = 0$$

and Eq. (12), for example, as

$$C_L(X_0, h) = \lambda[1 - S - \tfrac{1}{2}X_0] + \pi Sh/4 + I$$

where I denotes the term in Eq. (12) containing the integral. Then we suppose that, in the process of iteration, we find at some step a difference in the calculated value of C_L from that specified. Let this difference be ΔC_L. Then we have

$$\frac{\partial C_L}{\partial h}\Delta h + \frac{\partial C_L}{\partial X_0}\Delta X_0 = \Delta C_L$$

and

$$\frac{\partial G}{\partial h}\Delta h + \frac{\partial G}{\partial X_0}\Delta X_0 = 0$$

Evidently, one can solve for Δh and ΔX_0 and use them to determine the next value of h and X_0 in the iteration. The calculation of all the partial derivatives from the formulas of the preceding sections is rather tedious. We shall, therefore, proceed to the discussion of results.

Results

The first of these results is contained in Fig. 4 which shows the variation of L/D for a range of peak pressure locations at zero cavitation number. For each value of cavity thickness T three values of C_L are used. The Reynolds number of 1.3×10^6, chosen for this performance comparison, is in the range which is typical of Reynolds numbers of towing tank or water-tunnel tests. Note that the trends show that the nose loading, corresponding to large values of S, leads to more favorable L/D values than tail-loaded profiles, obtained at small values of S. Other trends illustrated in this figure, such as those of increasing L/D with increasing design C_L and the decrease of L/D with increasing cavity thickness, have been discussed in detail in Ref. 1. Therefore we shall conclude this discussion by considering some examples of profile geometry which result from the use of the present pressure distribution.

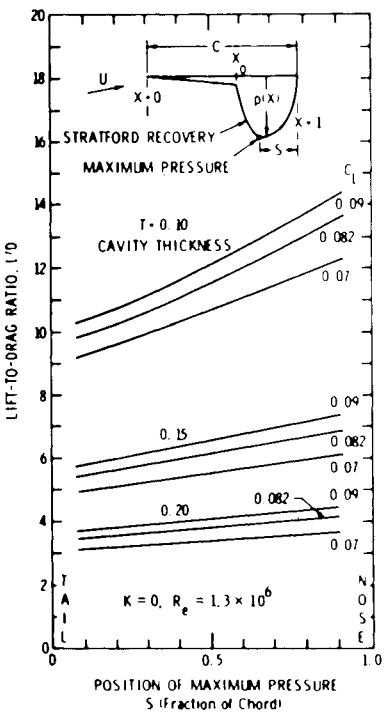

Fig. 4 Lift-to-drag ratio of profiles using Stratford recoveries for three prescribed lift coefficients and three cavity thicknesses. All profiles designed to operate at the ideal attack angle.

For these concluding examples, we shall consider a hydrofoil of 8 ft chord operating at 80 knots. The Reynolds number for this case is about 9×10^7. If the cavity is ventilated with air from the free surface, the cavitation number will be zero. On the other hand, if the submergence is about one chord length and the cavity contains water vapor, the cavitation number will be about 0.13. Actual values of K could lie between these extremes because the cavity will generally contain a mixture of air and vapor. Therefore, in our examples we will use $K=0$ and $K=0.13$ in order to illustrate these two bounding conditions. We will also take tail-loaded profiles corresponding to peak-pressure locations at $s=0.8$ and $s=0.9$ as measured from the hydrofoil nose. Thus, four profiles will be considered. All of them will be taken to have a cavity thickness parameter $T=0.1$ and a lift coefficient $C_L=0.12$. Figures 5-8 show the prescribed pressure distributions and the profile and cavity geometries which result at the "shockless entry" condition (first design procedure[1]).

In these illustrations, foil and cavity contours are shown in the upper part of each figure and the perturbation pressure distribution is plotted in the lower part. Note that the pressures are plotted as positive downward. The cavity contour between the nose and trailing edge of each profile is the upper curve in the foil-cavity plot. The wetted surface of the profile is the lower curve. The lower surface of the cavity

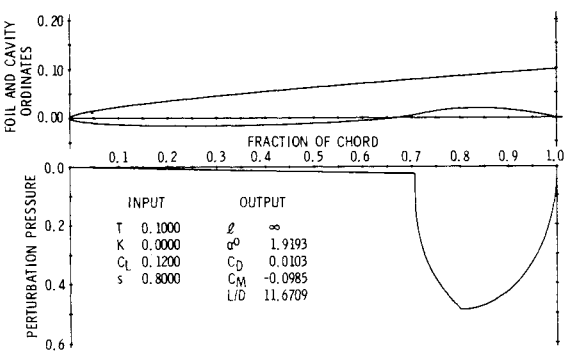

Fig. 5 Prescribed "Stratford-type" pressure distribution and cavity and wetted surface shapes at the ideal attack angle for a Reynolds number of 9×10^7.

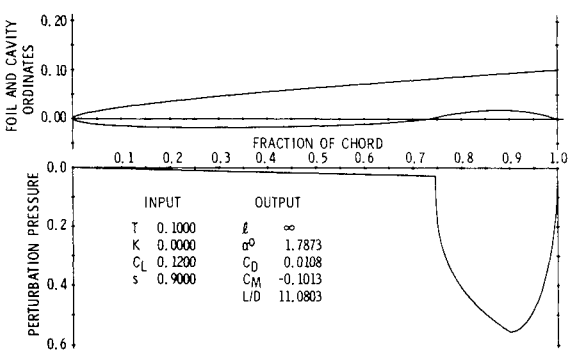

Fig. 6 Prescribed "Stratford-type" pressure distribution and cavity and wetted surface shapes at the ideal attack angle for a Reynolds number of 9×10^7.

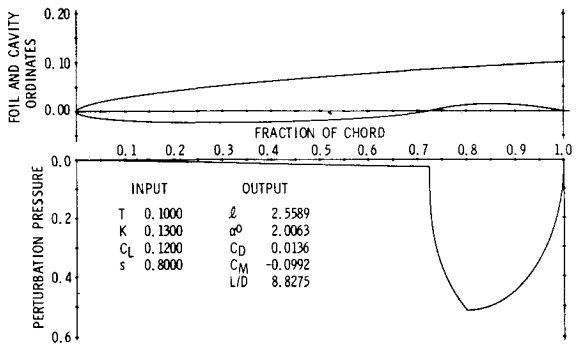

Fig. 7 Prescribed "Stratford-type" pressure distribution and cavity and wetted surface shapes at the ideal attack angle for a Reynolds number of 9×10^7.

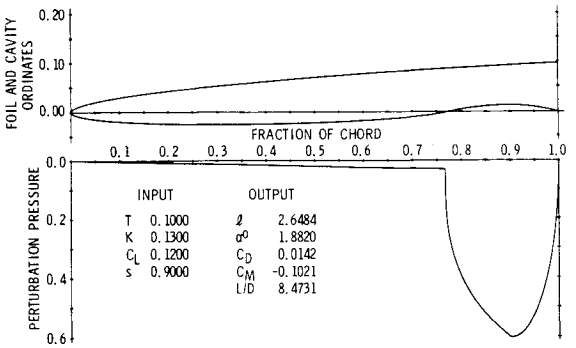

Fig. 8 Prescribed "Stratford-type" pressure distribution and cavity and wetted surface shapes at the ideal attack angle for a Reynolds number of 9×10^7.

which extends downstream from $X=1$, $Y=0$ is not shown at all.

For Figs. 5 and 6 in which $K=0$, it is seen that the pressure distribution becomes more sharply peaked as s increases from 0.8 to 0.9. The very rapid pressure rise provided by the Stratford recovery is clearly shown. Since both of these profiles have a design C_L of 0.12 the peak pressure at $s=0.9$ must be higher than that at $s=0.8$ and the chordwise distance occupied by the Stratford recovery for $s=0.9$ exceeds that for $s=0.8$. Figures 7 and 8 apply to $K=0.13$. When s is permitted to vary, the trends regarding prescribed pressures and cavity and foil geometries are essentially the same as those just described for the zero-cavitation-number case. On the other hand, comparison of Figs. 5 and 7 shows for $s=0.8$ that the peak pressure at $K=0.13$ and steepness of the pressure rise are greater than they are at $K=0$. Moreover the cavity and wetted surface contours are fatter when $K=0.13$ than they are when $K=0$, although in all cases the thickness at the trailing edge is $T=0.1$. Figures 6 and 8 which correspond to $s=0.9$ show the same trends with K as those just discussed for $s=0.8$. This thickening of foil and cavity with increasing K has been noted previously[1] and the reasons for this trend have been discussed.

Conclusions

In the foregoing paragraphs, we have adapted the Stratford pressure recovery for use in the design of tail-loaded supercavitating hydrofoil sections. Sections designed to operate at the ideal attack angle have been investigated. If the adverse pressure gradients are too severe, such sections could be subject to turbulent separation from the wetted surface. The use of the Stratford pressure rise for tail-loaded profiles can prevent unexpected turbulent separation and still permit one to concentrate the pressure loading very close to the trailing edge because the Stratford pressure rise is the steepest rise permissible with an attached turbulent boundary layer. The general hydrodynamic and geometric trends reported here are consistent with those reported previously but which were obtained for different pressure distributions and which did not consider possible turbulent separation. The profiles calculated are derived from linearized cavity flow theory. Therefore we expect them to be approximate shapes in much the same sense found by Liebeck and Ormsbee[5] when they did not use an exact inverse theory, although this deficiency was remedied later.[6] If a nonlinear parametric inverse design method for supercavitating hydrofoils had been used, the design process would be significantly improved. Nonetheless, the present considerations are useful for preliminary design. Promising candidates can be checked by nonlinear direct calculations and the most suitable candidate can be selected. The chief finding is that use of the Stratford recovery allows one to prescribe a very steeply increasing pressure indeed. Presumably, less steeply increasing pressure distributions will also be free of separation.

Acknowledgment

This work was supported by the Ships Performance Department, DTNSRDC under the Naval Material Command, Program Element 62544N, Task Area ZF43-421-110 and under the General Hydromechanics Research Program under contract N00017-73-C-1418. The author is grateful to Young Shen, and J.W. Holl for helpful discussions of this work and to R.F. Davis and J. Fernandez for assistance with the numerical work. The views expressed herein are strictly those of the author and do not necessarily reflect those of the David W. Taylor Naval Ship Research and Development Center.

References

[1] Parkin, B.R., Davis, R.F. and Fernandez, J., "Hydrodynamic Trends for Preliminary Design of Fully Cavitating Sections," *Marine Technology*, Vol. 14, Jan. 1977, p. 70.

[2] Parkin, B.R., Davis, R.F., and Fernandez, J., "A Numerical Design Study of Fully Cavitating Hydrofoil Sections Having Prescribed Pressure Distributions," Applied Research Laboratory Technical Memorandum, File No. TM 75-170, June 30, 1975, The Pennsylvania State University, Applied Research Laboratory, State College, PA, unlimited distribution.

[3] Stratford, B.S., "The Prediction of Separation of the Turbulent Boundary Layer," *Journal of Fluid Mechanics,* Vol. 5, Part 1, Jan. 1959, pp. 1-16.

[4] Stratford, B.S., "An Experimental Flow with Zero Skin Friction Throughout its Region of Pressure Rise," *Journal of Fluid Mechanics*, Vol. 5, Part 1, Jan. 1959, pp. 17-35.

[5] Liebeck, R.H. and Ormsbee, A.I., "Optimization of Airfoils for Maximum Lift," *Journal of Aircraft*, Vol. 7 Sept.-Oct. 1970, p. 409.

[6] Liebeck, R.H., "A Class of Airfoils Designed for High Lift in Incompressible Flow," *Journal of Aircraft*, Vol. 10, Oct. 1973, p. 610.

[7] Smith, A.M.O., "High-Lift Aerodynamics," *Journal of Aircraft*, Vol. 12, June 1975, p. 501.

[8] Smith, A.M.O., "Aerodynamics of High-Lift Airfoil Systems," AGARD Conference Preprint No. 102 on *Fluid Dynamics of Aircraft Stalling*, AGARD Conference Proceedings No. 4, May 1968.

[9] Cebeci, T., Mosinskis, G.T. and Smith, A.M.O., "Calculation of Separation Points in Incompressible Turbulent Flows," *Journal of Aircraft*, Vol. 9, Sept. 1972, p. 618.